Supporting Information

A Tale of Two Metal Ions: Contrasting Behaviors of High Oxidation States of Cu and Mn in Bicarbonate-H_2O_2 System

Zhiwei Yang[a,b], Xiaonan Tan[a], Daojian Tang[a], Jing Li[b], Jiahai Ma*[a]*

[a] School of Chemical Sciences, University of Chinese Academy of Sciences, Beijing 100049, P. R. China

[b] Chongqing Institute of Green and Intelligent Technology, Chinese Academy of Sciences, 100190, Beijing, P. R. China.

E-mail: majia@ucas.ac.cn

Table S1. Comparison of the current AOPs for successful treatment for azo dyes in some recent literature.

Ref.	AOPs	100% Degradation Time	Azo dyes
This work	metal ions intermediated bicarbonate-H_2O_2 system	10 min	congo red
1	Adsorption	15 min	methyl orange orange II congo red
2	Adsorption	60 min	reactive black 5 amaranth acid red 183
3	Synergistic Adsorption and Biodegradation	1400 min	orange II
4	Synergistic Adsorption and Photocatalysis	120 min	congo red
5	TiO_2 Photocatalysis	180 min	congo red
6	Fe−Cr Codoped $BaTiO_3$ Photocatalysis	100 min	methyl orange
7	Biodegradation	120 h	methyl orange Ponceau S Red
8	Bioelectrochemical System Integrated with a Membrane Biofilm Reactor	days	acid orange
9	Co Fenton-like system	50 min	sunset yellow
10	ozonation	30 min	methyl orange
11	Catalytic reduction by Ag and Au nanoparticles stabilized on graphene oxide functionalized with PAMAM dendrimers)	3 min	methyl orange congo red
12	Reduction by mediated Sulfide	50 min	methyl orange

References.

1. M. Chaaban, H. El-Rassy, Nickel−Aluminum Oxide Aerogels: Super-adsorbents for Azo Dyes for Water Remediation. ACS Omega. 5 (2020) 27401-27412.
2. M. Vall, M. Strømme, O. Cheung, Amine-Modified Mesoporous Magnesium Carbonate as an Effective Adsorbent for Azo Dyes. ACS Omega. 4 (2019) 2973-2979.
3. M. Ahmad, M. Yousaf, A. Nasir, I. Ah. Bhatti, A. Mahmood, X. Fang, X. Jian, K. Kalantar-Zadeh, N. Mahmood, Porous Eleocharis@MnPE Layered Hybrid for Synergistic Adsorption and Catalytic Biodegradation of Toxic Azo Dyes from Industrial Wastewater. Environ. Sci. Technol. 53 (2019) 2161−2170.
4. X. Liu, T. Zhu, Y. Gong, Efficient Removal of Azo-Dyes in Aqueous Solution by CeB_6 Nanocrystals. ACS Appl. Nano Mater. 2 (2019) 5704−5712.
5. J. A. Bumpus, J. Tricker, K. Andrzejewski, H. Rhoads, M. Tatarko, Remediation of Water Contaminated with an Azo Dye: An Undergraduate Laboratory Experiment Utilizing an Inexpensive Photocatalytic Reactor. J. Chem. Edu. 76 (1999) 1680-1683.
6. I. C. Amaechi, A. H. Youssef, D. Rawach, J. P. Claverie, S. Sun, A. Ruediger, Ferroelectric Fe−Cr Codoped BaTiO3 Nanoparticles for the Photocatalytic Oxidation of Azo Dyes. ACS Appl. Nano Mater. 2 (2019) 2890−2901.
7. D. Baena-Baldiris, A. Montes-Robledo, R. Baldiris-Avila, *Franconibacter sp.,* 1MS: A New Strain in Decolorization and Degradation of Azo Dyes Ponceau S Red and Methyl Orange. ACS Omega. 5 (2020) 28146-28157.
8. Y. Pan, T. Zhu, Z. He, Enhanced Removal of Azo Dye by a Bioelectrochemical System Integrated with a Membrane Biofilm Reactor. Ind. Eng. Chem. Res. 57 (2018) 16433−16441.
9. Z. Li, L. Wang, M. Tian, Z. Li, Z. Yuan, C. Lu. Tris−Co(II)−H_2O_2 System-Mediated Durative Hydroxyl Radical Generation for Efficient Anionic Azo Dye Degradation by Integrating Electrostatic Attraction. ACS Omega. 4 (2019) 21704-21711.
10. C. Feng , P. Diao, Nickel foam supported $NiFe_2O_4$-NiO hybrid: A novel 3D porous catalyst for efficient heterogeneous catalytic ozonation of azo dye and nitrobenzene. Applied Surface Science 541 (2021) 148683.

11. R. Rajesh, S. S. Kumarb, R. Venkatesan, Efficient degradation of azo dyes using Ag and Au nanoparticles stabilized on graphene oxide functionalized with PAMAM dendrimers. New J. Chem. 38 (2014) 1551-1558.
12. H. Zhao, S. Huang, W. Xu, Y. Wang, Y. Wang, C. He, Y. Mu, Undiscovered Mechanism for Pyrogenic Carbonaceous Matter-Mediated Abiotic Transformation of Azo Dyes by Sulfide. Environ. Sci. Technol. 53 (2019) 4397−4405.

Table S2. Characteristic peak wavelength of selected dyes. Conditions: dyes 0.02 mM, metal ions

dyes	CR	MBH	MO	RB	RhB	RR
Characteristic peak (nm)	494	665	465	545	554	543

0.1 mM, HCO_3^- 40 mM, H_2O_2 10 mM.

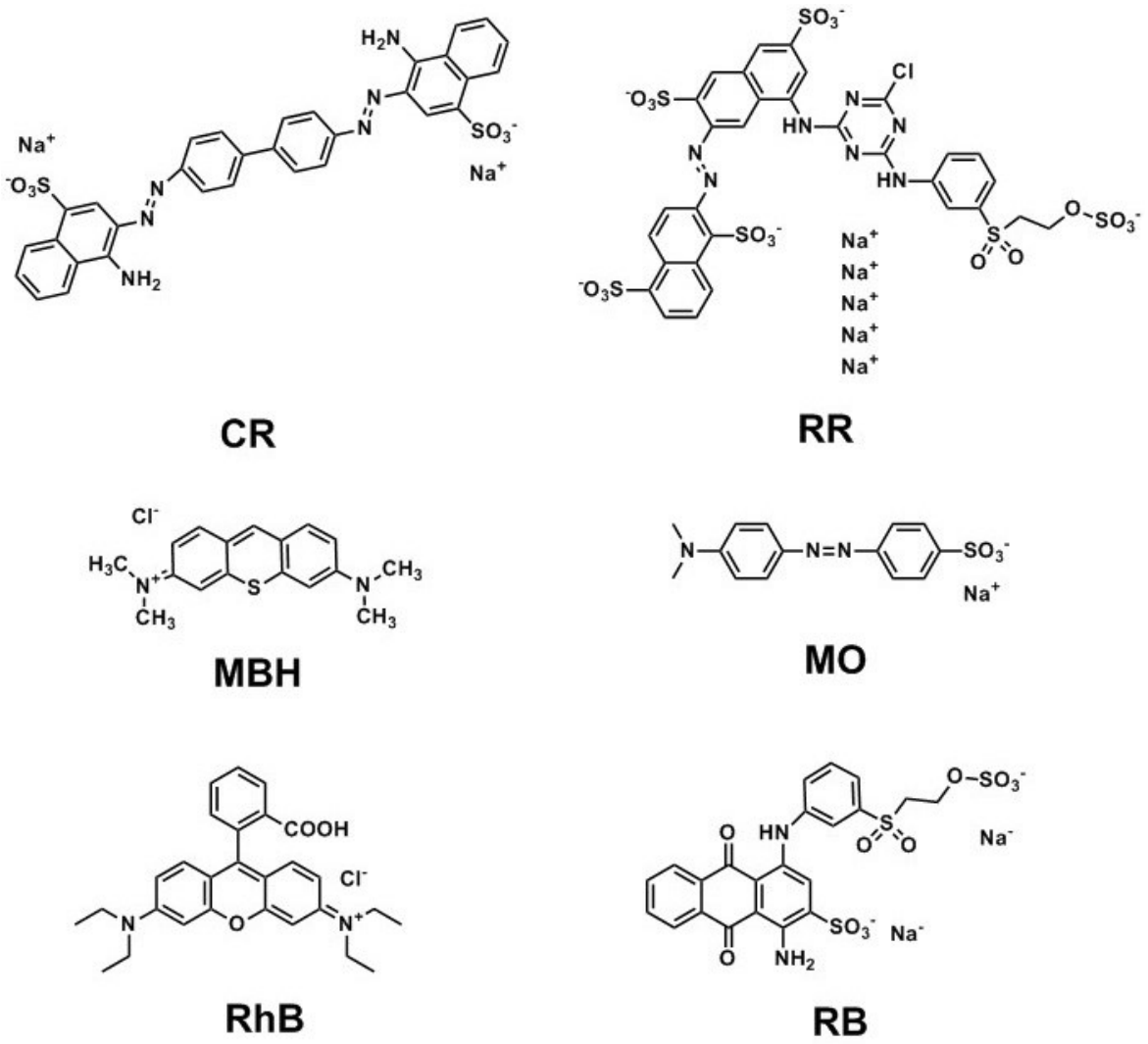

Scheme S1. Structural formula of selected six dyes.

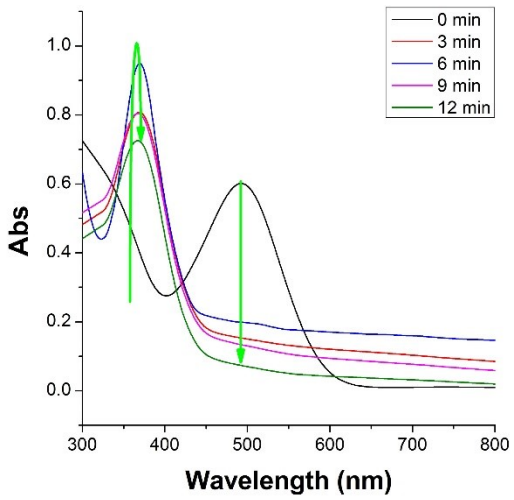

Figure S1. The Uv-Vis spectrum of CR during degradation. Conditions: CR 0.02 mM, Cu^{2+} 0.1 mM, HCO_3^- 40 mM, H_2O_2 10 mM.

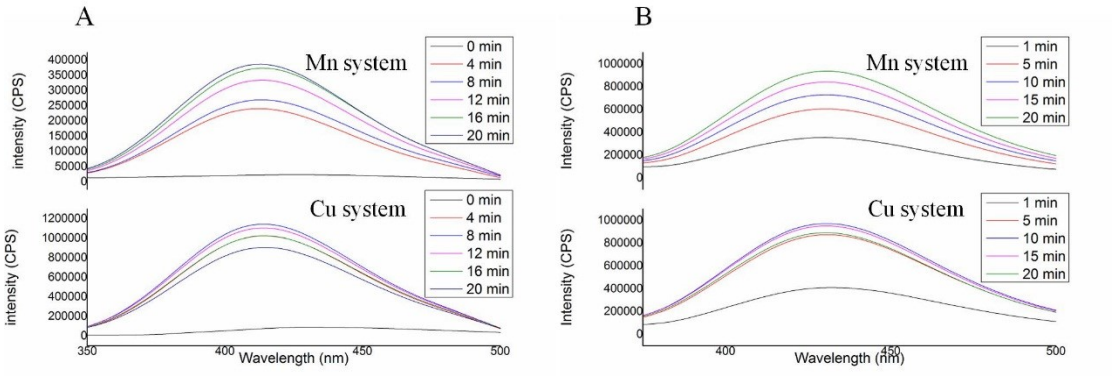

Figure S2. Fluorescence spectra analysis of (A) BA as fluorescent probe and (B) TA as fluorescent probe. Conditions: Cu^{2+} 0.1 mM, Mn^{2+} 0.1 mM, HCO_3^- 40 mM, H_2O_2 10 mM, BA 0.3 mM, TA 0.3mM. excitation wavelength 287 nm.

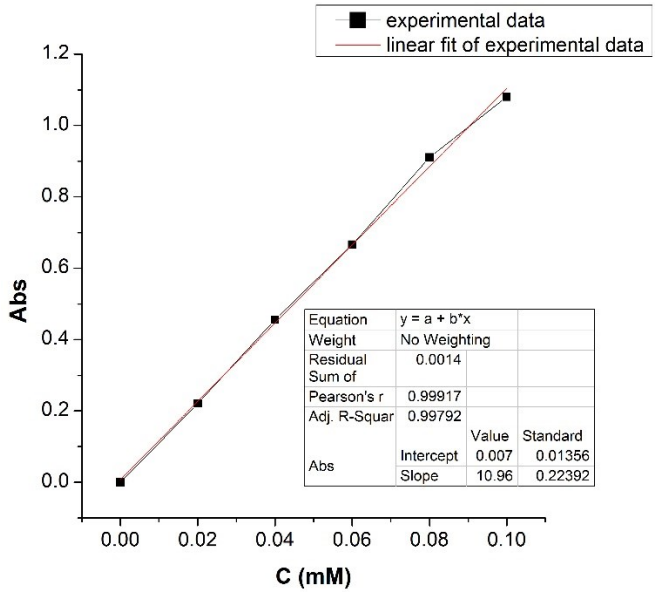

Figure S3. The linear relationship between Abs and concentration of Cu (Ⅰ) by bathocuproine.

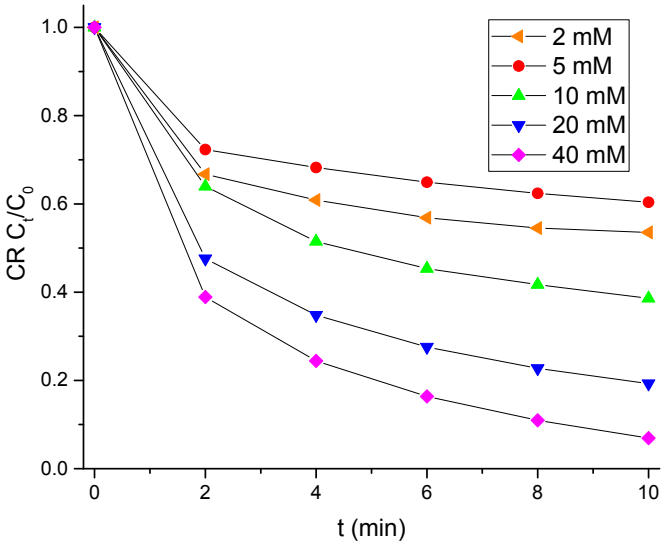

Figure S4. The dosage effect of o bicarbonate. Conditions: CR 0.02 mM, Cu^{2+} 0.1 mM, H_2O_2 10 mM.

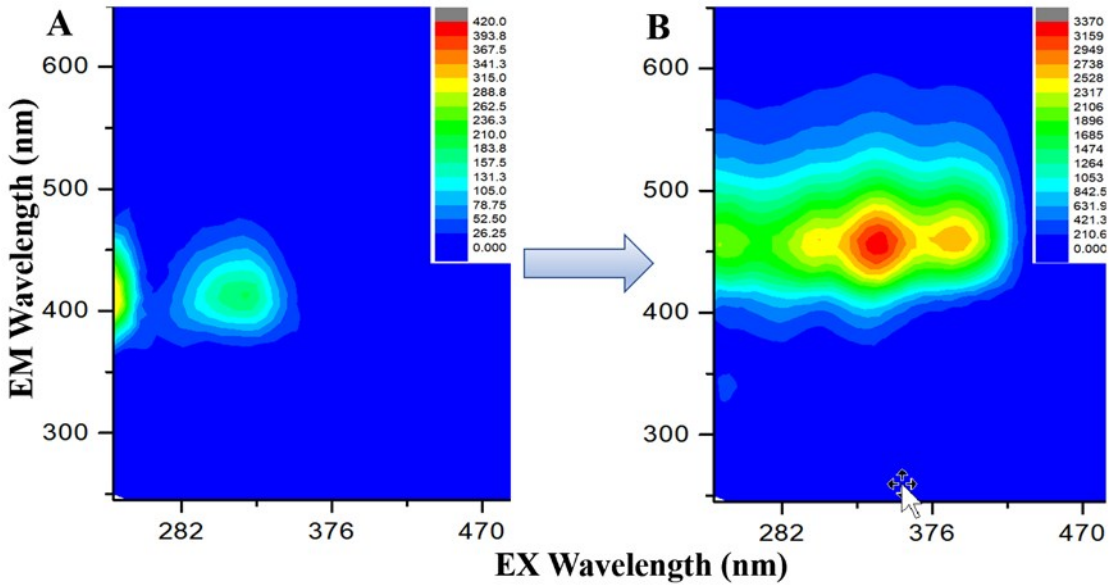

Figure S5. The 3D fluorescence spectra of CR. A: before the reaction; B: after the reaction. Conditions: CR 0.02 mM, Cu^{2+} 0.1 mM, HCO_3^- 40 mM, H_2O_2 10 mM.